

# Patterns of conductivity in excitable automata with updatable intervals of excitations

Andrew Adamatzky

*University of the West of England, Bristol, UK*

We define a cellular automaton where a resting cell excites if number of its excited neighbours belong to some specified interval and boundaries of the interval change depending on ratio of excited and refractory neighbours in the cell's neighbourhood. We calculate excitability of a cell as a number of possible neighbourhood configurations that excite the resting cell. We call cells with maximal values of excitability conductive. In exhaustive search of functions of excitation interval updates we select functions which lead to formation of connected configurations of conductive cells. The functions discovered are used to design conductive, wire-like, pathways in initially non-conductive arrays of cells. We demonstrate that by positioning seeds of growing conductive pathways it is possible to implement a wide range of routing operations, including reflection of wires, stopping wires, formation of conductive bridges and generation of new wires in the result of collision. The findings presented may be applied in designing conductive circuits in excitable non-linear media, reaction-diffusion chemical systems, neural tissue and assemblies of conductive polymers.

## I. INTRODUCTION

Excitable cellular automata are well endowed tools for studying complex phenomena of spatio-temporal physical, chemical and biological systems [1, 2], prototyping of chemical media [3, 4], reaction-diffusion computers [5], studying calcium wave dynamics [6], and chemical turbulence [7].

In a classical Greenberg-Hasting [8] automaton model of excitation a cell takes three states — resetting, excited and refractory. A resting cell becomes excited if number of excited neighbours exceeds a certain threshold, an excited cell becomes refractory, and a refractory cell returns to its original resting state. In [9] we introduced a bit more exotic cellular automaton, where a resting cell is excited if a number of its excited neighbours belongs to some fixed interval  $[\theta_1, \theta_2]$ . The interval  $[\theta_1, \theta_2]$  is called an excitation interval. For a two-dimensional cellular automaton with eight-cell neighbourhood boundaries of the excitation interval are between 1 and 8:  $1 \leq \theta_1 \leq \theta_2 \leq 8$ . By tuning  $\theta_1$  and  $\theta_2$  we control automata dynamics and evoke target and spiral waves, stationary excitation patterns, and mobile localisations [5].

How does excitation dynamics change if we allow boundaries of the excitation interval to change during the automaton development? We partially answered the question in [10] by making the interval  $[\theta_1^t(x), \theta_2^t(x)]$  of every cell  $x$  dynamically updatable at every step  $t$  depending on state of the cell  $x$  and numbers of excited and refractory neighbours in the cell  $x$ 's neighbourhood. We found that excitable cellular automata with dynamical excitation intervals exhibit a wide range of space-time dynamics based on an interplay between propagating excitation patterns and excitability of cells modified by the excitation patterns. Such interactions lead to formation of standing domains of excitation, stationary waves and localised excitations. We analysed morphological and generative diversities of the functions studied and characterised the functions with highest values of the diversities.

Excitable cellular automata with dynamical intervals of excitation can be considered as discrete phenomenological models, or rather conceptual analogs, of memristive media and excitable chemical medium computers.

### A. Memristive medium

The memristor — a passive resistor with memory — is a device whose resistance changes depending on the polarity and magnitude of a voltage applied to the device's terminals and the duration of this voltage's application. Its existence was theoretically postulated by Leon Chua in 1971 based on symmetry in integral variations of Ohms laws [11–13]. The first experimental prototypes of memristors are reported in [14–16]. An importance, and the great pragmatic value, of memristors is that one can design logically universal, or functionally complete, circuits composed entirely of the memristors. Potential unique applications of memristors are in spintronic devices, ultra-dense information storage, neuro-morphic circuits [17], and programmable electronics [18], designing binary arithmetical circuits with polymer organic memristors [19].

Despite phenomenal number of results in memristors produced literally every week there are insufficient findings on phenomenology of spatially extended non-linear media with hundreds of thousands of locally connected memristive elements. Three cellular automaton models of a memristive medium were suggested so far:

- Itoh-Chua memristor cellular automata, where cellular automaton lattice is actually designed of memristors [20],

- Adamatzky-Chua model of memristive cellular automata based on structurally-dynamic cellular automata [21],
- semi-memristive automata [22].

Itoh-Chua and Adamatzky-Chua models imitate memristive properties of links, connections between cells of automata arrays but not the cells themselves. The semi-memristive automata bring memristivity into cells [22]: links between cells are always 'conductive' but cells themselves can take non-conductive, or refractory, states. The semi-memristive automata are excitable cellular automata with retained refractoriness.

In present paper, an excitability of a cell is calculated as a number of possible neighbourhood configurations that excite the resting cell. *Cells with maximal values of excitability are called conductive.* We represent conductivity of a cell  $x$  via boundaries of its excitation interval  $[\theta_1(x), \theta_2(x)]$ . We excite the cellular automaton, wait till the perturbation spreads and boundaries of excitation intervals of cells updated and then select cells with highest values of excitability. The configurations of conductive cells form conductive pathways by analogy with the formation of conductive pathways in disordered networks of organic memristors [23]. In automata studied polarity of a direct current applied to a cell  $x$  is imitated by excited and refractory neighbours of  $x$ , and current intensity is represented by a ratio of excited and refractory neighbours.

## B. Ensembles of Belousov-Zhabotinsky vesicles

Excitable reaction-diffusion computers, especially those based on Belousov-Zhabotinsky reaction, employ principles of a collision-based computing [5]. Wave-fragments collide in a 'free' space and change their velocity vectors in the result the collision. When input and output waves are interpreted as logical variables, the site of the waves' collision can be seen as a logical gates. Wave-fragments, similar to dissipative solitons [24], are inherently unstable: they either collapse or explode. A way to overcome the problem of wave-fragments' instability was suggested in [25–27]: a subdivision of the computing substrate into interconnected compartments, so called BZ-vesicles, and allowing waves to collide only inside the compartments. Each BZ-vesicle has a membrane that is impassable for excitation. A pore, or a channel, between two vesicles is formed when two vesicles come into direct contact. The pore is small such that when a wave passes through the pore there is insufficient time for the wave to expand or collapse before interacting with other waves entering through adjacent pores, or sites of contact.

It has been observed in chemical laboratory experiments with BZ-vesicles [28] that waves of oxidation induced by external stimulation, e.g. with a silver wire, propagating in the initially resting BZ medium may cause changes in the excitability of BZ-vesicles (not just refractoriness but excitability in a long run). Excitability of BZ-vesicles can increase after first round of the oxidation wave propagation. A cellular automaton model designed in present paper gives a phenomenological snapshot of an ensemble of regularly arranged BZ-vesicles (imitated by cells), which change their long-term excitability after being subjected to propagating waves of excitation.

The paper is structured as follows. We define an excitable cellular automata with dynamically updated boundaries of excitation interval in Sect. II. Configurations of conductivity generated by the automata are analysed in Sect. III. The functions which produce fully conductive configurations are selected in exhaustive search. Section IV demonstrates how to design conductive wire-like pathways by positions seeds of excitation. Potential further developments are outlined in Sect. V.

## II. EXCITATION CONTROLLED EXCITATION INTERVALS

Let  $L$  be a two-dimensional orthogonal array of finite state machines, or cells,  $x^t$  and  $x^{t+1}$  states of a cell  $x$  at time steps  $t$  and  $t+1$ , and  $\sigma_+^t(x)$  a sum of excited neighbours in cell  $x$ 's eight-cell neighbourhood  $u(x) = \{y : |x-y|_{L_\infty} = 1\}$ . Cell  $x$  updates its state by the following rule,  $x^{t+1} = f(u(x))$ , where cell-state update function  $f$  is represented as

$$x^{t+1} = \begin{cases} +, & \text{if } x^t = \circ \text{ and } \sigma_+^t(x) + \in [\theta_1^t(x), \theta_2^t(x)] \\ -, & \text{if } x^t = + \\ \circ, & \text{otherwise} \end{cases} \quad (1)$$

A resting cell is excited if a number of its neighbours belongs to excitation interval  $[\theta_1^t(x), \theta_2^t(x)]$ , where  $1 \leq \theta_1^t(x), \theta_2^t(x) \leq 8$ . The boundaries  $\theta_1^t(x)$  and  $\theta_2^t(x)$  are dynamically updated depending on cell  $x$ 's state and numbers of  $x$ 's excited  $\sigma_+^t(x)$  and refractory  $\sigma_-^t(x)$  neighbours. A natural way to update boundaries is by increasing or decreasing their values as follows:

$$\begin{aligned} \theta_1^{t+1}(x) &= \xi(\theta_1^t(x) + \Delta_1 \phi(\sigma_+^t(x) - \sigma_-^t(x))) \\ \theta_2^{t+1}(x) &= \xi(\theta_2^t(x) + \Delta_2 \phi(\sigma_+^t(x) - \sigma_-^t(x))) \end{aligned} \quad (2)$$

where

$$\Delta_1 = \begin{cases} T_1, & \text{if } x = + \\ T_3, & \text{if } x = - \\ 0, & \text{if } x = 0 \end{cases} \quad \Delta_2 = \begin{cases} T_2, & \text{if } x = + \\ T_4, & \text{if } x = - \\ 0, & \text{if } x = 0 \end{cases} \quad (3)$$

and  $\phi(a - b) = 1$  if  $a > b$ , 0 if  $a = b$  and -1 if  $a < b$ , and  $\xi(a) = 1$  if  $a < 1$  and 8 if  $a > 8$ . Boundaries of excitation interval  $[\theta_1^t(x), \theta_2^t(x)]$  are updated independently of each other. Rules of excitation intervals update are determined by values of  $T_1, \dots, T_4$ . We therefore address the functions as tuples  $E(T_1, T_2, T_3, T_4)$  which range from  $E(-1, -1, -1, -1)$  to  $E(1, 1, 1, 1)$ .

Excitability  $\mathcal{E}(\theta_1(x), \theta_2(x))$  of a cell  $x$  with excitation interval  $[\theta_1(x), \theta_2(x)]$  is measured as a number of all possible local configurations which have sum of excited cells lying in the excitation interval  $[\theta_1(x), \theta_2(x)]$ :

$$\mathcal{E}(\theta_1, \theta_2) = |\{w \in \{\circ, +, -\}^8 : f(w) = +\}| \quad (4)$$

Two highest excitability values are reached by cells with excitation intervals  $[1, 7]$  and  $[1, 8]$ ,  $\mathcal{E}(1, 7) = 6304$  and  $\mathcal{E}(1, 8) = 6305$ . We assume a cell  $x$  is conductive if  $\mathcal{E}(\theta_1(x), \theta_2(x)) > 6300$ . Connectivity of the configurations of cells with maximal excitability is considered to be analog of conductivity of the whole cellular array. The connectivity is estimated using standard bucket fill algorithm.

**Definition 1** We call conductivity configuration diameter  $D$  fully conductive if there is a path between two sites lying at distance  $D$  from each other, and over 90% of sites are reached from any given site.

We study formation of conductive pathways in initially non-conductive medium. Therefore, in experiments we considered initial conditions  $\theta_1^0(x) = 2$  and  $\theta_2^0(x) = 8$  for any  $x$ . The excitation interval  $[2, 8]$  gives a cell excitability 5281, which is below a threshold adopted as indicator of conductivity.

We excite a disc radius 200 cells with a random configuration of excited states. Let  $p$  be a probability for a cell  $x$  to be assigned excited state at  $t = 0$  and one of its neighbours, chosen at random, also assigned an excited state. Two neighbouring excited cells is a minimal size of perturbation due to  $\theta_1^0(x) = 2$ . We considered  $p = 10^{-3}$  and  $p = 0.1$ . Initially cells inside a disc radius 200 are assigned excited states with probability  $p$ .

In each trial we allowed the cellular automaton to develop for 440 iterations and then analysed configurations of conductivity. Size of cellular arrays was chosen large enough for a front of perturbation to never reach the array's boundaries in 440 steps, so there are no influences of boundary conditions.

### III. CONDUCTIVE CONFIGURATIONS

Sites of initial random excitations generate waves, localizations and other travelling patterns of excitation. The patterns either stay localised or merge and propagate outwards the initially perturbed region. The patterns of excitation update boundaries of excitation intervals of cells they excited. An example of cellular automaton, function  $E(-1, 1, 0, -1)$ , development is shown in Fig. 1. Waves of excitation propagate from the perturbation sites (Figs. 1a and 2), leaving somewhat fibre-like trails and extended domains of lower  $\theta_1$  (Fig. 1b) and upper  $\theta_2$  (Fig. 1c) boundaries of excitation interval. These are reflected in solid domains of conductivity partially linked with wire-like conductive paths (Fig. 1d). Excitation waves originated from different sites of perturbation merge outside the stimulation disc and propagate further as almost connected packet of target waves (Fig. 1a). These waves leave triangular solid domains of conductivity behind (Fig. 1d).

#### A. Classes of connectivity

We characterise local connectivity of conductivity configurations using  $\nu_{\max}$ , a number of conductive neighbours of a conductive cell occurred most frequently in the configuration of conductivity, and  $\nu_{\min}$ , occurred less frequently. For initial probability of excitation  $10^{-3}$  we have twelve classes of local connectivity, the functions are grouped by values  $\mathcal{N} = (\nu_{\max}, \nu_{\min})$  of their conductivity configurations. Examples of configurations of conductivity generated by functions from these classes are shown in Figs. 3 and 4.

- $\mathcal{N} = (0, 0)$ :  $E(0, -1, 0, -1)$ ,  $E(0, -1, 0, 0)$ ,  $E(0, -1, 0, 1)$ ,  $E(0, 0, 0, -1)$ ,  $E(0, 0, 0, 0)$ ,  $E(0, 0, 0, 1)$ ,  $E(0, 1, 0, -1)$ ,  $E(0, 1, 0, 0)$ ,  $E(0, 1, 0, 1)$ .

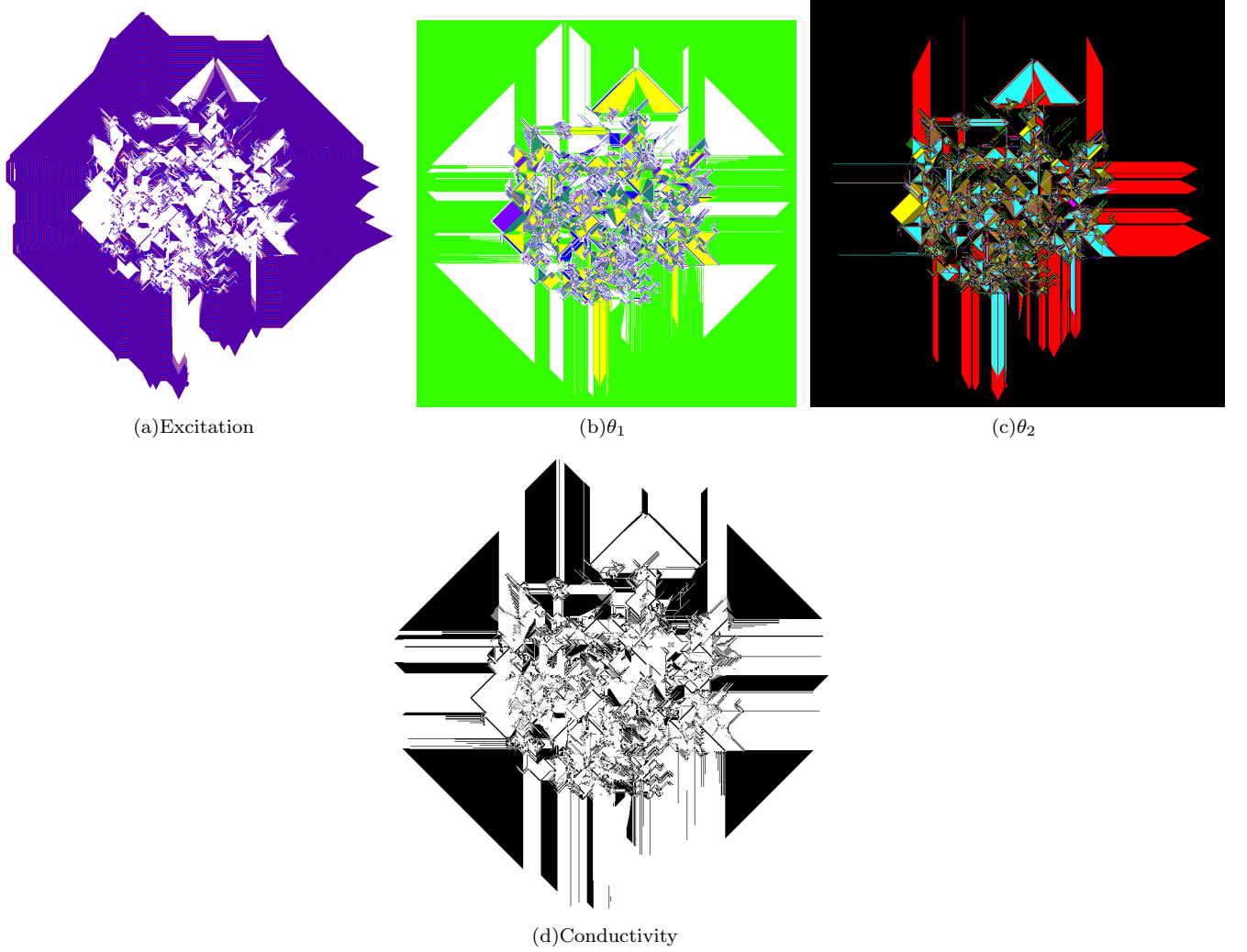


FIG. 1: (Color online) Snapshots of (a) excitation pattern, (b) configuration of lower boundary  $\theta_1$  of excitation interval, (c) configuration of upper boundary  $\theta_2$  of excitation interval, (d) configuration of conductivity of cellular automaton governed by function  $E(-1, 1, 0, -1)$ . Array of  $880 \times 880$  cells evolved for 440 steps. Initially cells inside a disc radius 200 are assigned excited states with probability  $10^{-3}$ . Cell states in (a) are represented by colours and grey levels as follows: excited state  $+$  is red (c. 76 grey), resting state is white and refractory state  $-$  is blue (c. 28 grey). Colour values of excitation interval boundaries  $\theta_1$  (b) and  $\theta_2$  (c) are following: 1 is white, 2 is green or 150 grey, 3 is yellow or 226 grey, 4 is blue or 28 grey, 5 is magenta or 104 grey, 6 is cyan or 178 grey, 7 is red or 76 grey, and 8 is black. Conductive cells in (d) are black and non-conductive are white.

- $\mathcal{N} = (0, 4)$ :  $E(1, 0, 0, -1)$ ,  $E(1, 1, 0, -1)$  (Fig. 3a)
- $\mathcal{N} = (2, 5)$ :  $E(0, -1, 1, 1)$  and  $E(1, 1, 0, 0)$  (Fig. 3b)
- $\mathcal{N} = (2, 6)$ :  $E(1, 1, 0, 1)$  (Fig. 3c)
- $\mathcal{N} = (2, 7)$ :  $E(0, 0, 1, 1)$ ,  $E(0, 1, 1, 1)$ ,  $E(1, -1, 0, -1)$ ,  $E(1, -1, 1, -1)$ ,  $E(1, -1, 1, 0)$ ,  $E(1, -1, 1, 1)$ ,  $E(1, 0, 1, -1)$ ,  $E(1, 0, 1, 0)$ ,  $E(1, 0, 1, 1)$ ,  $E(1, 1, 1, -1)$ ,  $E(1, 1, 1, 0)$ ,  $E(1, 1, 1, 1)$  (Fig. 3d)
- $\mathcal{N} = (2, 8)$ :  $E(0, -1, 1, -1)$ ,  $E(0, -1, 1, 0)$ ,  $E(0, 0, 1, -1)$ ,  $E(0, 0, 1, 0)$ ,  $E(0, 1, 1, -1)$ ,  $E(0, 1, 1, 0)$  (Fig. 3e)
- $\mathcal{N} = (5, 0)$ :  $E(1, -1, 0, 1)$ ,  $E(1, 0, 0, 1)$  (Fig. 3f)
- $\mathcal{N} = (7, 0)$ :  $E(1, -1, 0, 0)$ ,  $E(1, 0, 0, 0)$  (Fig. 4a)

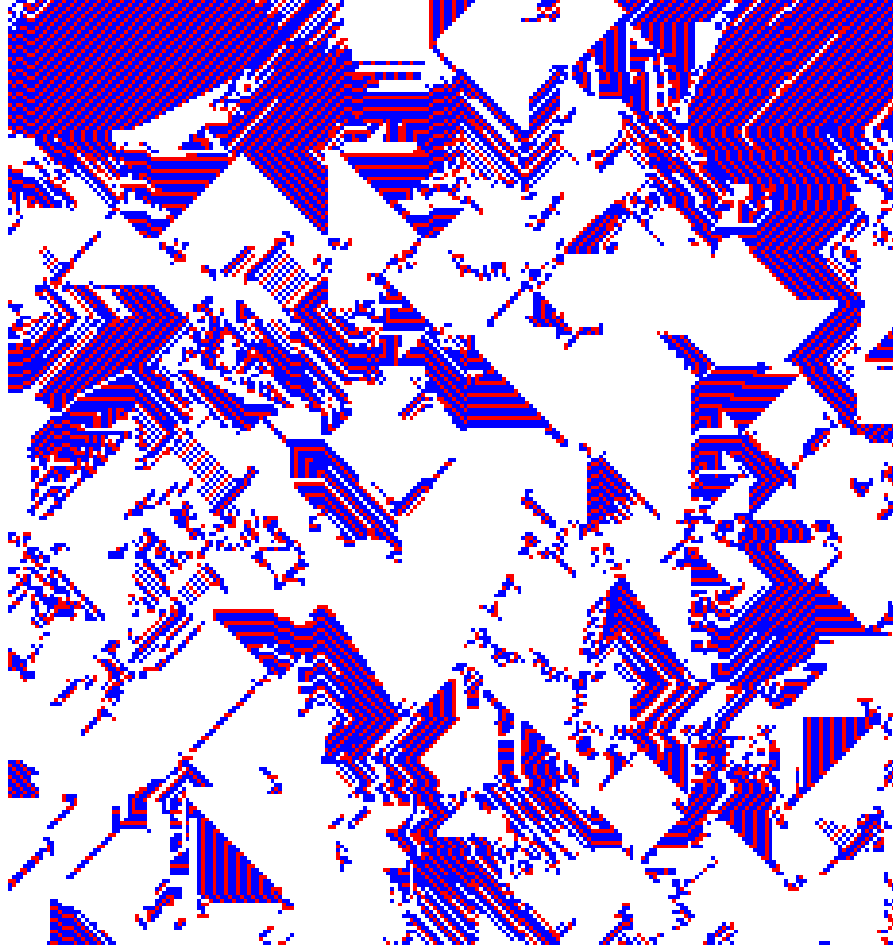


FIG. 2: (Color online) Enlarged part of excitation pattern from Fig. 1a

- $\mathcal{N} = (8, 0)$ :  $E(-1, -1, -1, -1)$ ,  $E(-1, -1, 1, 1)$ ,  $E(-1, 0, -1, -1)$ ,  $E(-1, 0, 0, -1)$ ,  $E(-1, 0, 0, 0)$ ,  $E(-1, 1, 0, -1)$ ,  $E(-1, 1, 0, 0)$ ,  $E(-1, 1, 0, 1)$ ,  $E(0, -1, -1, -1)$ ,  $E(0, -1, -1, 0)$ ,  $E(0, -1, -1, 1)$ ,  $E(0, 0, -1, 0)$ ,  $E(0, 0, -1, 1)$ ,  $E(0, 1, -1, 1)$ ,  $E(1, -1, -1, -1)$ ,  $E(1, -1, -1, 0)$ ,  $E(1, -1, -1, 1)$ ,  $E(1, 0, -1, 0)$ ,  $E(1, 1, -1, 1)$  (Fig. 4b)
- $\mathcal{N} = (8, 1)$ :  $E(-1, -1, -1, 0)$ ,  $E(-1, -1, -1, 1)$ ,  $E(-1, 0, -1, 0)$ ,  $E(-1, 0, -1, 1)$ ,  $E(-1, 1, -1, 0)$ ,  $E(-1, 1, -1, 1)$ ,  $E(1, 0, -1, 1)$  (Fig. 4c)
- $\mathcal{N} = (8, 3)$ :  $E(-1, -1, 0, 0)$ ,  $E(-1, -1, 0, 1)$ ,  $E(-1, -1, 1, 0)$ ,  $E(-1, 0, 1, 1)$ ,  $E(-1, 1, -1, -1)$ ,  $E(-1, 1, 1, 1)$ ,  $E(0, 0, -1, -1)$ ,  $E(0, 1, -1, -1)$ ,  $E(0, 1, -1, 0)$ ,  $E(1, 0, -1, -1)$ ,  $E(1, 1, -1, -1)$ ,  $E(1, 1, -1, 0)$  (Fig. 4d)
- $\mathcal{N} = (8, 6)$ :  $E(-1, -1, 0, -1)$ ,  $E(-1, -1, 1, -1)$ ,  $E(-1, 0, 0, 1)$ ,  $E(-1, 0, 1, -1)$ ,  $E(-1, 0, 1, 0)$ ,  $E(-1, 1, 1, -1)$ ,  $E(-1, 1, 1, 0)$  (Fig. 4e)

Class  $\mathcal{N} = (8, 0)$  is the largest class, it has 19 functions. Configurations of conductivity generated by the functions from  $\mathcal{N} = (8, 0)$  (Fig. 4b) are characterised by large solid conductive domains formed either by initial source of excitation, see e.g. rectangular embedded shapes in Fig. 4b, or by merging fronts of excitation (solid polygonal domains at the periphery).

The next largest classes are  $\mathcal{N} = (2, 7)$  and  $\mathcal{N} = (8, 3)$  (Fig. 4d). Each of them includes 12 functions. Conductivity configurations generated by functions of class  $\mathcal{N} = (2, 7)$  consist mainly of isolated line segments of cells in conductive states and pairs or singletons. Configurations generated by functions of  $\mathcal{N} = (8, 3)$  are comprised of solid domains of conductive states and sparsely scattered singletons (Fig. 3d).

Classes  $\mathcal{N} = (2, 5)$  (Fig. 3b),  $\mathcal{N} = (2, 6)$  (Fig. 3c) and  $\mathcal{N} = (2, 7)$  (Fig. 3d) pose particular interest because majority of conductive cells have two conductive neighbours each and therefore chances of conductive 'wires' to be formed could be high.

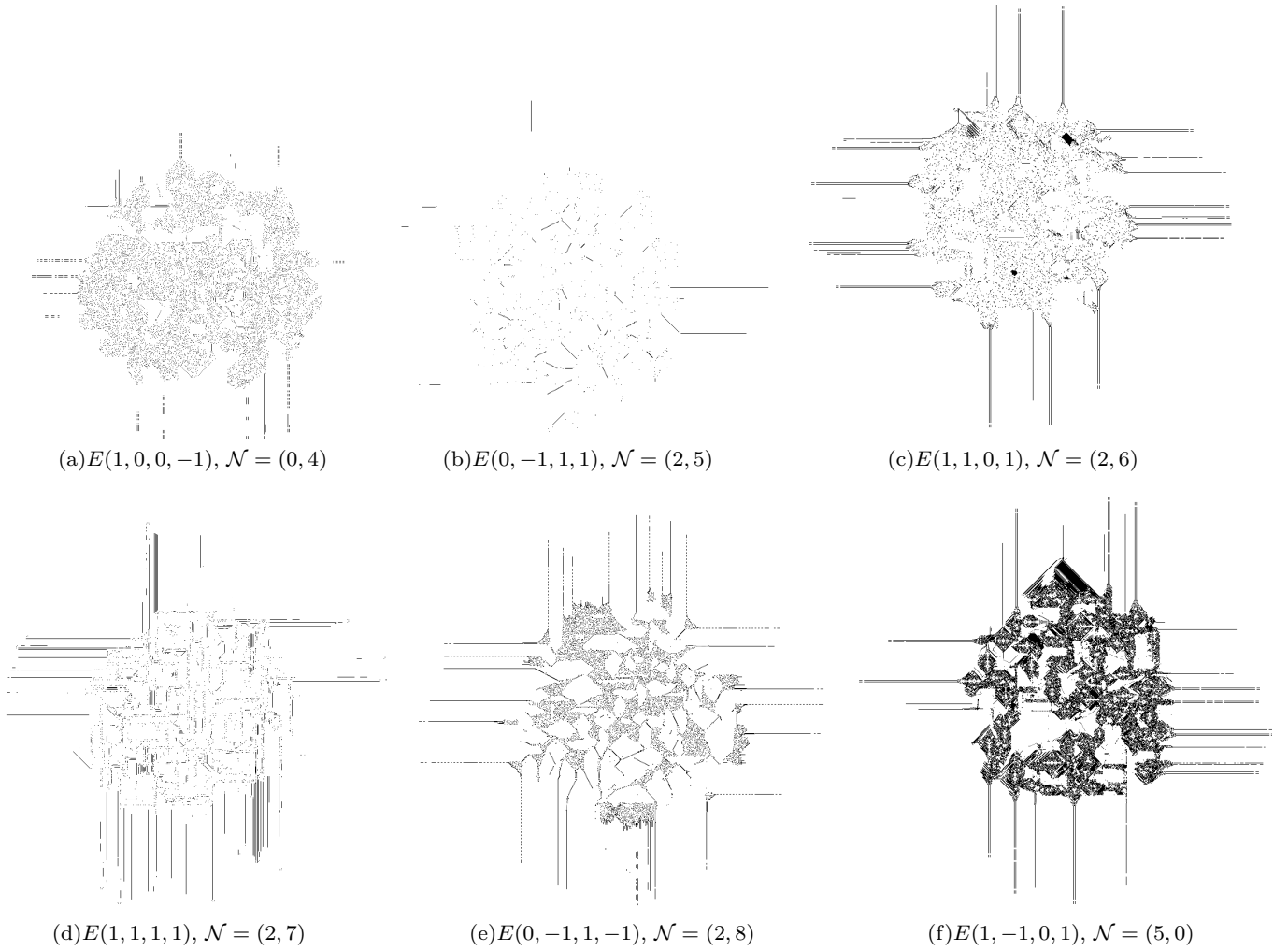


FIG. 3: Examples of conductivity configurations.

Configurations generated by functions from  $\mathcal{N} = (2,5)$  (Fig. 3b) predominantly consist of singletons and pairs of cells in conductive states; the pairs are aligned in staircase like fashion but there is no immediate connection between the pairs (Fig. 5a). There are zig-zag like 'wires' of conductive states (Fig. 5b) in configurations (Fig. 3c) generated by the only function  $E(1,1,0,1)$  in class  $\mathcal{N} = (2,6)$ . However they are present as isolated fragments. Configurations (Fig. 3e) generated by function  $E(0,1,1,0)$  of class  $\mathcal{N} = (2,8)$  consist of clusters of singletons — single conductive cells surrounded by non-conductive neighbours — and pairs of cells in conductive states. The clusters are connected to each other with diagonals of singletons (Fig. 5c). Neither of the functions with  $\nu_{max} = 2$  generate fully conductive configurations but few functions from classes  $\mathcal{N} = (7,0)$  and  $\mathcal{N} = (8,0)$  do. We study these functions below.

### B. Functions generating conductive configurations

Most functions generate only partially conductive configurations of conductivity. Examples of connected clusters are shown in Fig. 6.

**Finding 1** For low probability of initial excitation,  $p = 10^{-3}$ , functions  $E(1,0,0,0)$  and  $E(1,-1,0,0)$  generate fully conductive configurations. For high probability of initial excitations,  $p = 0.1$ , fully conductive configurations are generated by functions  $E(-1,0,0,0)$  and  $E(-1,1,0,0)$ .

For low probability  $p = 10^{-3}$  of initial excitation only functions  $E(1,-1,0,0)$  (Figs. 7a) and  $E(1,0,0,0)$  generate fully conductive configurations. For initial configurations with high probability of excited cells ( $p = 0.1$ ) only two

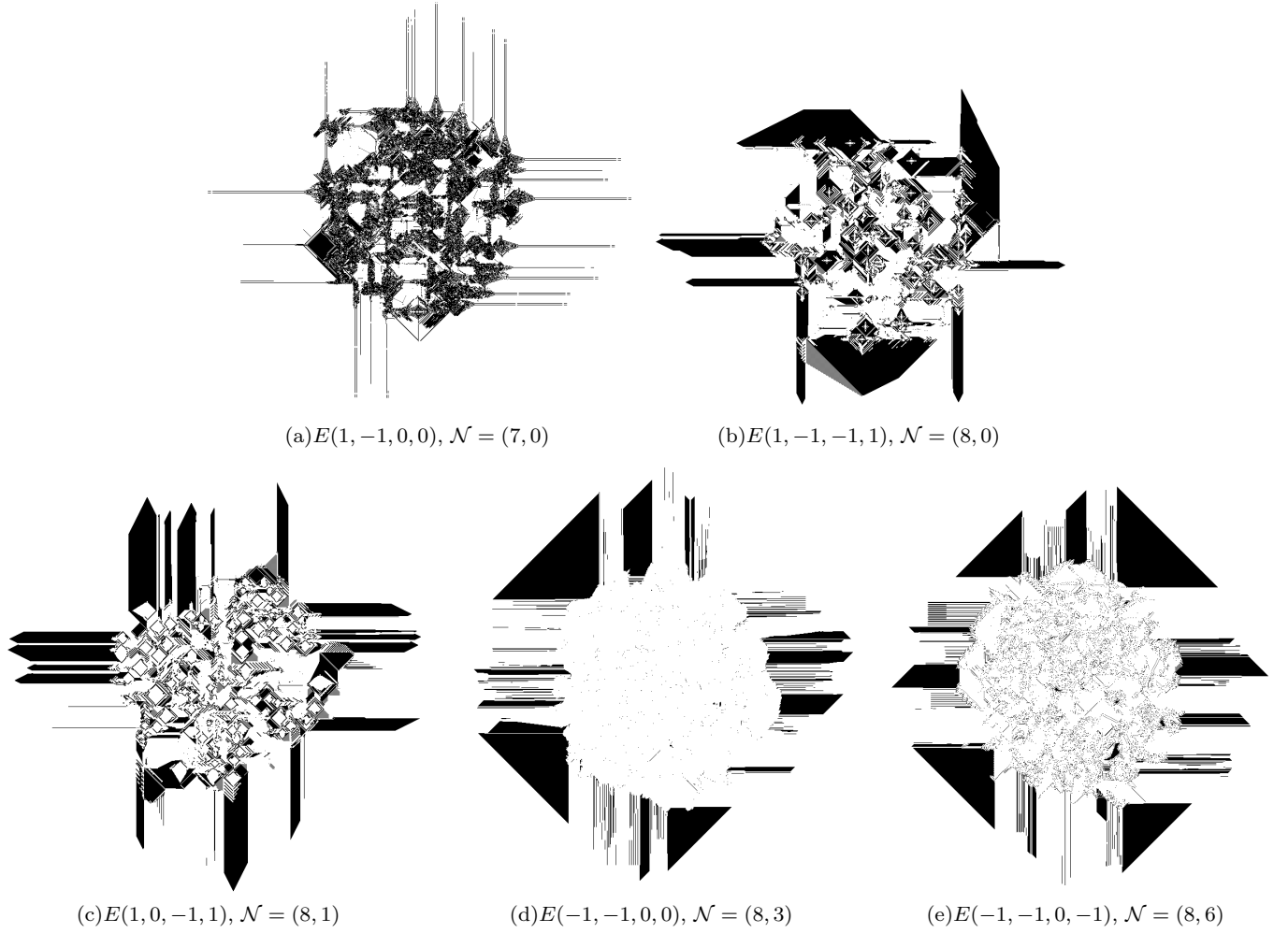


FIG. 4: Examples of conductivity configurations.

functions generate conductive configurations:  $E(-1, 0, 0, 0)$  (Fig. 7c) and  $E(-1, 1, 0, 0)$  (Fig. 7d). In all four functions selected values  $T_3$  and  $T_4$  are nil. The values correspond to update of excitation intervals of refractory cells. This is in line with commonly accepted assumption that in an excitable medium elements in refractory state are insensitive to states of their neighbours. Mechanics of excitation interval updates of excited cells is illustrated in Fig. 8.

Function  $E(1, 0, 0, 0)$  increases lower boundary  $\theta_1(x)$  of excitability interval of a cell  $x$  when a number of excited neighbours of the cell exceeds a number of refractory neighbours. If a cell has less excited neighbours than refractory ones then lower boundary of the excitability interval decreases. Function  $E(1, -1, 0, 0)$  increases lower boundary  $\theta_1$  and decreases upper boundary  $\theta_2$  of excitability interval of a cell when excited neighbours of the cells are in majority. If refractory cells dominate in a cell's neighbourhood then  $\theta_1$  decreases and  $\theta_2$  increases (Fig. 8). Both functions decrease excitability of a cell when the cell's neighbourhood is 'over-excited' (prevalence of excited neighbours) and increase the cell's excitability when the cell's neighbourhood 'over-refractory' (prevalence of refractory neighbours). Thus they stabilise the excitation dynamics.

Function  $E(-1, 0, 0, 0)$  decreases  $\theta_1$  when a cell has majority of excited neighbours and increases  $\theta_1$  if refractory neighbours dominate. Function  $E(-1, 1, 0, 0)$  expands excitation interval ( $\theta_1$  decreases and  $\theta_2$  increases) when there are more excited than refractory neighbours; and contracts the excitation interval ( $\theta_1$  increases and  $\theta_2$  decreases) when refractory neighbours prevail (Fig. 8). The functions increase excitability of cells with 'over-excited' neighbourhoods and decrease excitability of cells with 'over-refractory' neighbourhoods. Thus they destabilise the excitation dynamics.

**Finding 2** For low probabilities of initial perturbations functions stabilising excitation dynamics generate conductive configurations while for high probabilities of initial perturbations functions de-stabilising excitation dynamics generate conductive configurations.

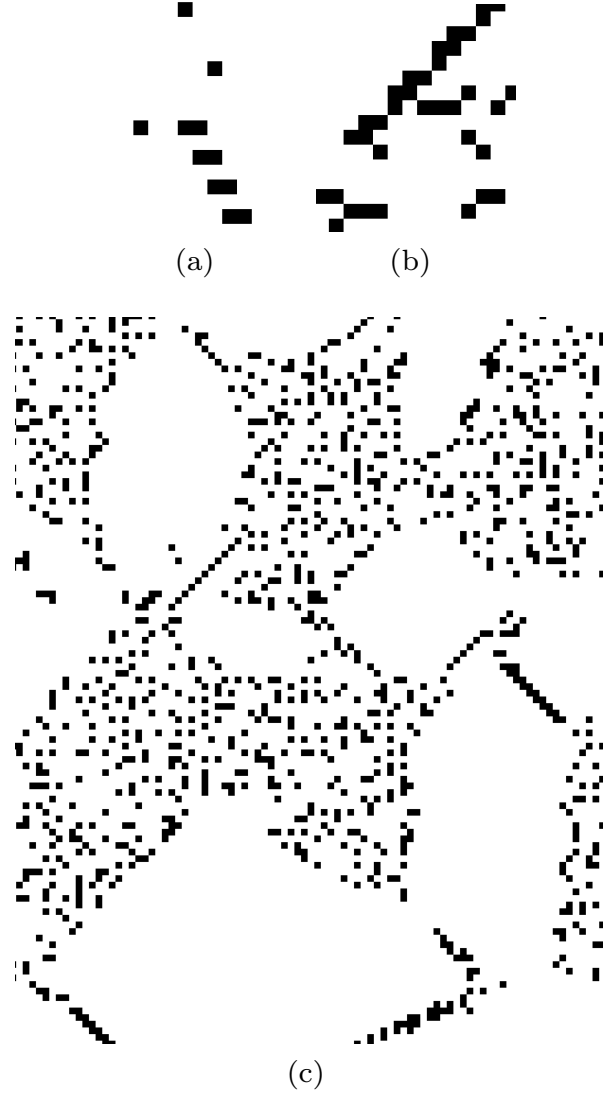


FIG. 5: Fragments of configurations generated by (a) function  $E(0, -1, 1, 1)$  from  $\mathcal{N} = (2, 5)$ , (b) function  $E(1, 1, 0, 1)$  from  $\mathcal{N} = (2, 6)$ , (c) function  $E(0, 1, 1, 0)$  from  $\mathcal{N} = (2, 8)$ .

Let  $E(e_1, e_2, e_3, e_4)$  be a function generating conductive configurations for low probability of excitation in initial configurations and  $E'(e'_1, e'_2, e'_3, e'_4)$  the function generating conductive configurations for high probability of excitation in initial configuration. Then

$$E(e_1, e_2, e_3, e_4) = E'(-1 \cdot e'_1, -1 \cdot e'_2, -1 \cdot e'_3, -1 \cdot e'_4)$$

#### IV. GROWING CONDUCTIVE PATHWAYS WITH FUNCTIONS $E(1 - 100)$ AND $E(1000)$

Let us consider how to route conductive pathways using minimal resources. The pathways can be initiated by exciting the medium. A minimal seed is a pair of cells in excited state  $++$  or  $\begin{smallmatrix} + \\ + \end{smallmatrix}$ . The seed generates a growing pattern of excitation (Fig. 9). The excitation pattern starts as a target wave (Fig. 9c-f). At sixth step of development excitation ruptures inside the wave-front on its eastmost and westmost sites (Fig. 9g), and propagates along the wave-front boundary inside the target wave (Fig. 9h-j). At tenth step of the seed's development the excitation reaches the original seed's position (Fig. 9k). Thus the propagating pattern becomes 'filled' with persistent excitation activity.

The associated development of configurations of cells in conductive state is shown in Fig. 10. The seed initiates two

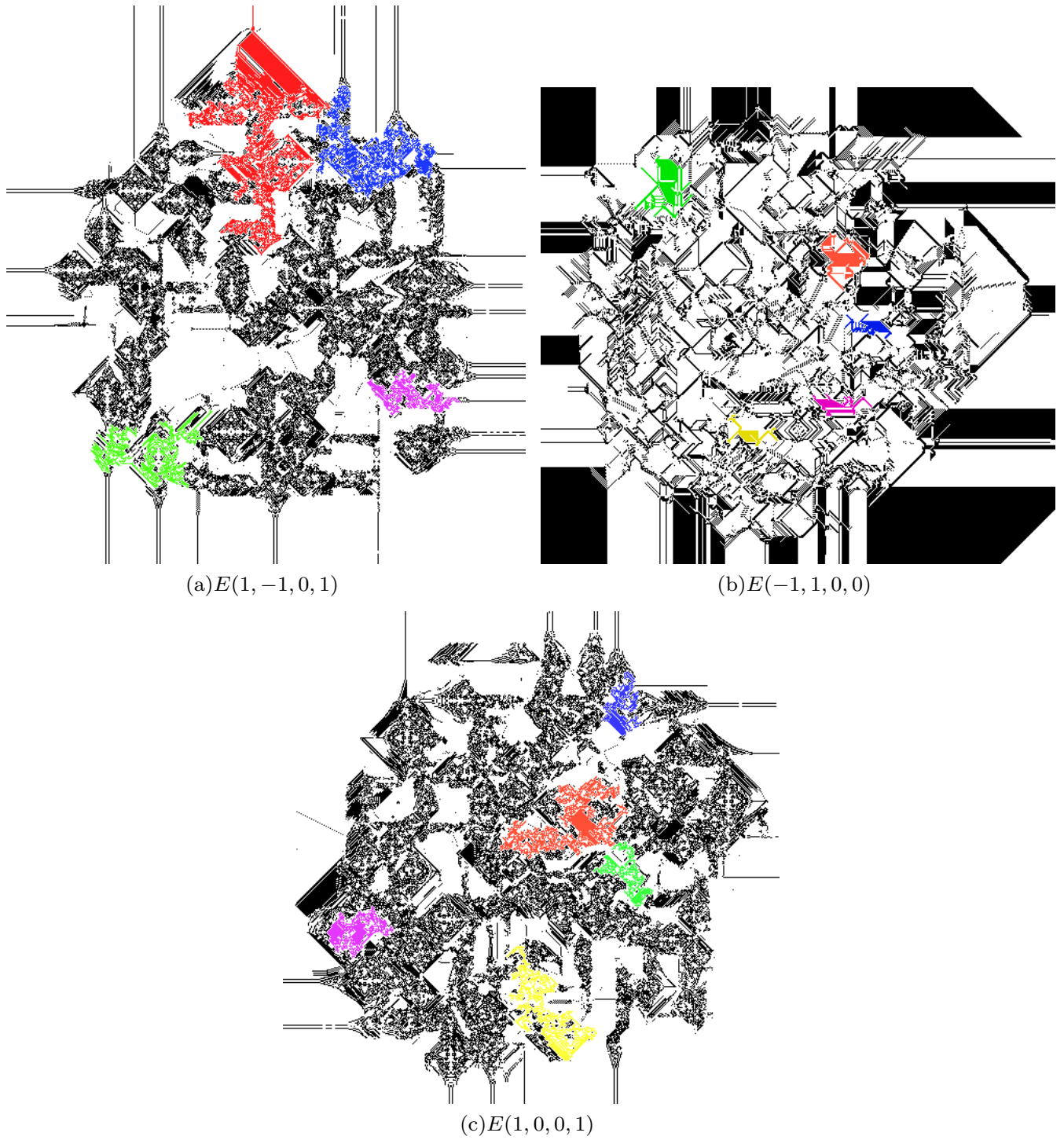


FIG. 6: (Color online) Examples of configurations with partially connectivity clusters coloured. The clusters are bucket flooded with red, blue, green, magenta and yellow colours (seen as shades of grey in black and white reproduction).

types of growing pathways: single chains and double chains of conductive states. For example, a configuration evoked by seed  $++$  (Fig. 9a) exhibits two single chains, growing west and east, and two double chains, growing north and south Fig. 10. The chains growing north and south increase their lengths by one one cell each, speed 1. The chains growing west and east increase by one cell every other step of development, speed  $1/2$ .

The mechanics of formation of conductive pathways is illustrated in Fig. 11. Excited cells having configurations

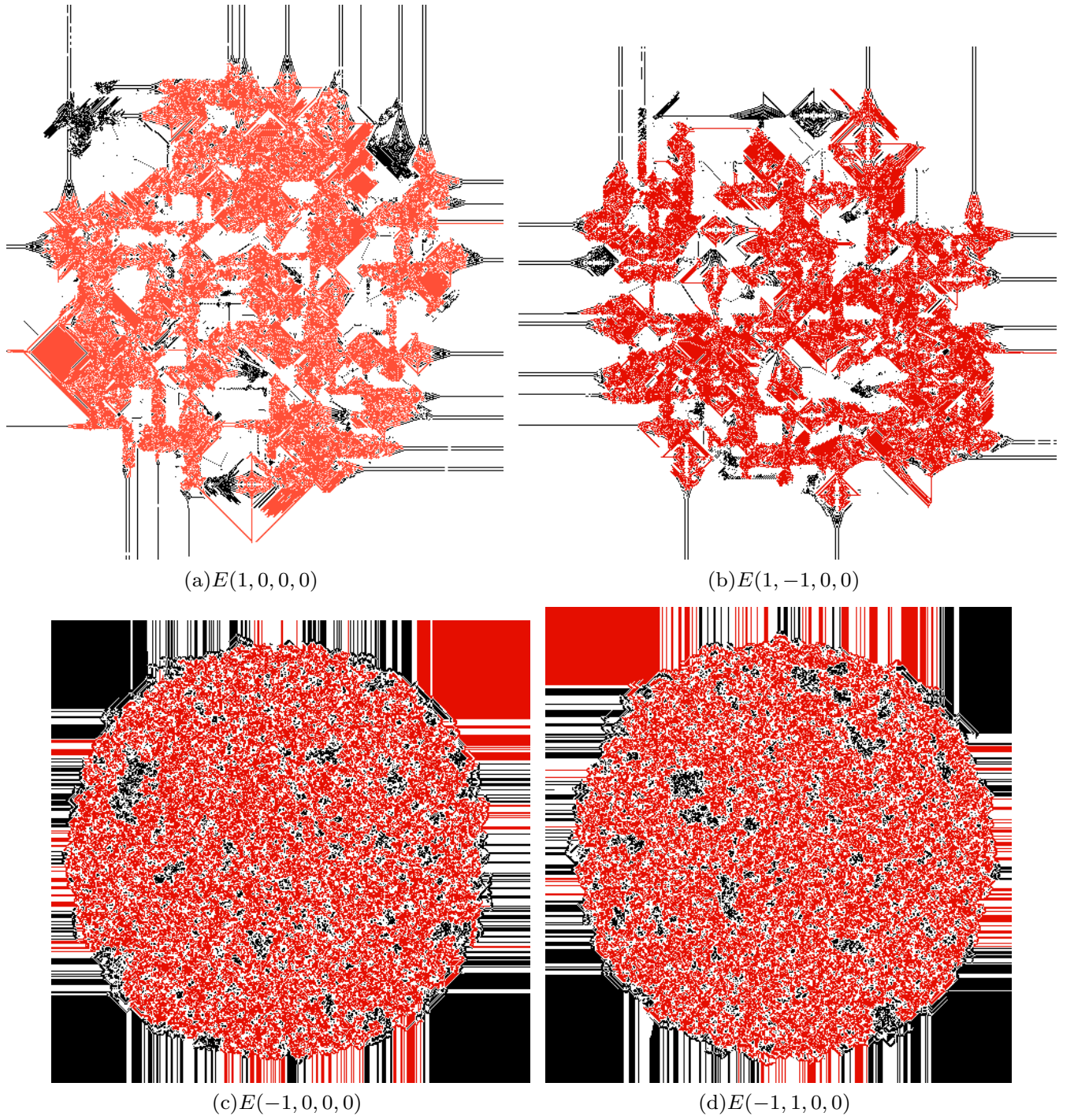


FIG. 7: (Color online) Examples of conductivity configurations generated by functions (a)  $E(1, 0, 0, 0)$ , (b)  $E(1, -1, 0, 0)$ , (c)  $E(-1, 0, 0, 0)$  and (d)  $E(-1, 1, 0, 0)$ . Non-conductive cells are white. Instances of connected clusters of conductive cells are bucket flooded with red (c. 76 grey).

$\begin{smallmatrix} \circ & \circ & - \\ \circ & + & \circ \\ \circ & - & \circ \end{smallmatrix}$  and  $\begin{smallmatrix} - & \circ & \circ \\ \circ & + & \circ \\ \circ & - & \circ \end{smallmatrix}$  (north and south proximities of the excitation pattern), and configurations  $\begin{smallmatrix} \circ & \circ & - \\ \circ & + & \circ \\ - & \circ & \circ \end{smallmatrix}$  and  $\begin{smallmatrix} - & \circ & \circ \\ \circ & + & \circ \\ \circ & - & \circ \end{smallmatrix}$  (west and east proximities of the excitation patterns) decrease their values of  $\theta_1(x)$  from 2 to 1, thus increasing the cells' excitability.

**Finding 3** By positioning an additional cell in excited or refractory state nearby the original seed of two excited cells it is possible to generate a wide range of single thread wires growing into pre-determined directions.

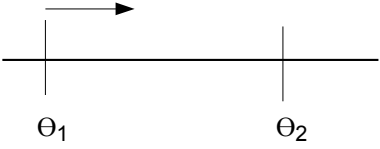
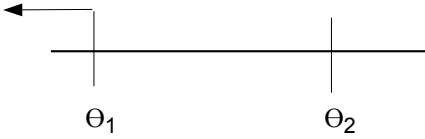
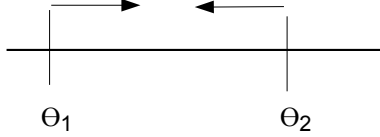
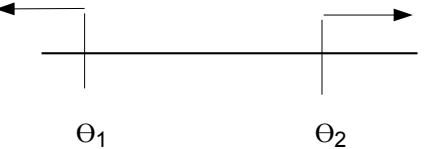
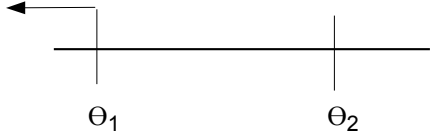

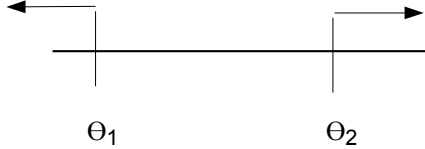
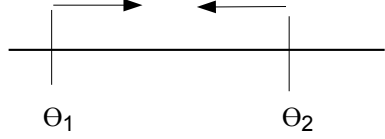
$p$	$T_1$	$T_2$	$\sigma_+ > \sigma_-$	$\sigma_+ < \sigma_-$
$10^{-3}$	1	0		
	-1	1		
$10^{-1}$	-1	0		
	-1	1		

FIG. 8: Mechanics of excitation interval update in functions  $E(1, 0, 0, 0)$ ,  $E(1, -1, 0, 0)$ ,  $E(-1, 0, 0, 0)$  and  $E(-1, 1, 0, 0)$ .  $\sigma_+$  is a number of excited neighbours in a cell's neighbourhood and  $\sigma_-$  is a number of refractory neighbours.

Let us consider several examples.

If we excite a cell above east site of the seed  $\begin{smallmatrix} \circ & \circ \\ + & + \end{smallmatrix}$  the modified seed  $\begin{smallmatrix} + & \circ \\ + & + \end{smallmatrix}$  will develop into a growing excitation pattern which generates two chains of cells in conductive states. One chain grows east and another chain grows south. Space-time configurations of excited and refractory cells and conductive cells are shown in Fig. 12. A seed of three excited cells (Fig. 12a) develops into an excitation wave fragment propagating south-east (Fig. 12egi). The wave-fragment expands east and south (Fig. 12kmo) and resembles an oxidation wave-fragment in sub-excitable Belousov-Zhabotinsky medium [5]. Conductive wires are produced at the sites of excited cells, which have neighbourhood configurations  $\begin{smallmatrix} \circ & \circ & \circ \\ \circ & + & \circ \\ - & \circ & \circ \end{smallmatrix}$  (north corner of the expanding wave fragment) and  $\begin{smallmatrix} \circ & - & \circ \\ \circ & + & \circ \\ - & \circ & \circ \end{smallmatrix}$  (south corner) (Fig. 12kmo).

To produce three wires growing north, south and east we excite a neighbouring cell north-west of the seed  $\begin{smallmatrix} + & + \end{smallmatrix}$  (Fig. 13). The configuration  $\begin{smallmatrix} \circ & \circ & + \\ + & + & + \end{smallmatrix}$  of initial excitation generates a wave-fragment of excited and refractory states which travels west and expands north and south (Fig. 13ikmo). A wire growing west is produced by decreasing  $\theta_1$  of excited cell with neighbourhood  $\begin{smallmatrix} + & \circ & - \\ - & + & \circ \\ + & \circ & - \end{smallmatrix}$  because it has more refractory neighbours (three cells) than excited neighbours (two cells). Wires growing north and south are produced by excited cells having neighbourhood configurations  $\begin{smallmatrix} \circ & \circ & - \\ \circ & + & \circ \\ \circ & - & \circ \end{smallmatrix}$  and  $\begin{smallmatrix} \circ & - & \circ \\ \circ & + & \circ \\ \circ & - & \circ \end{smallmatrix}$ .

By making north neighbour of eastern excited cell of the seed  $\begin{smallmatrix} + & + \end{smallmatrix}$  refractory we produce a single chain of conductive cells growing south (Fig. 14). The pattern  $\begin{smallmatrix} - & \circ \\ + & + \end{smallmatrix}$  (Fig. 14a) is transformed into a particle of three excited and three

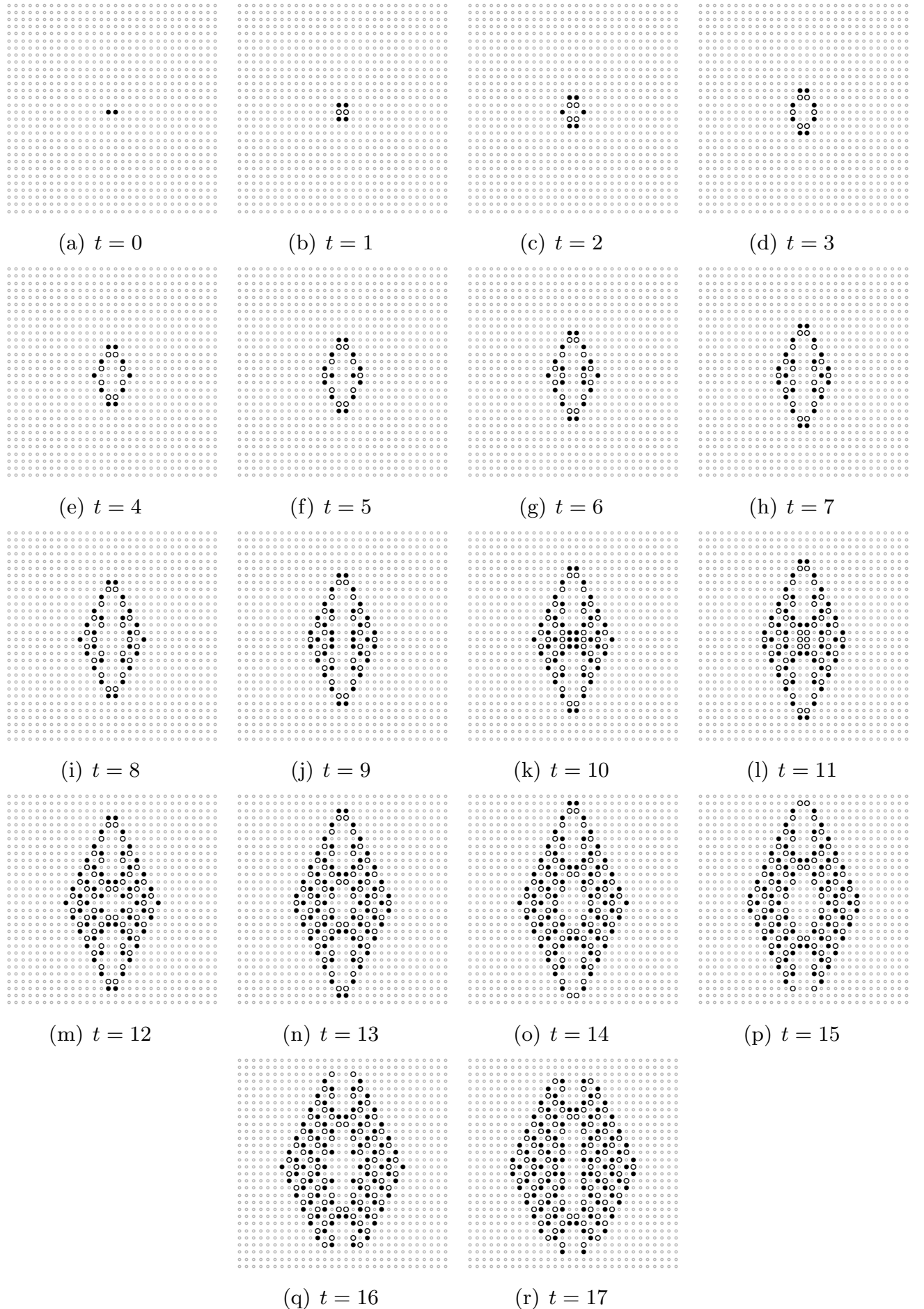
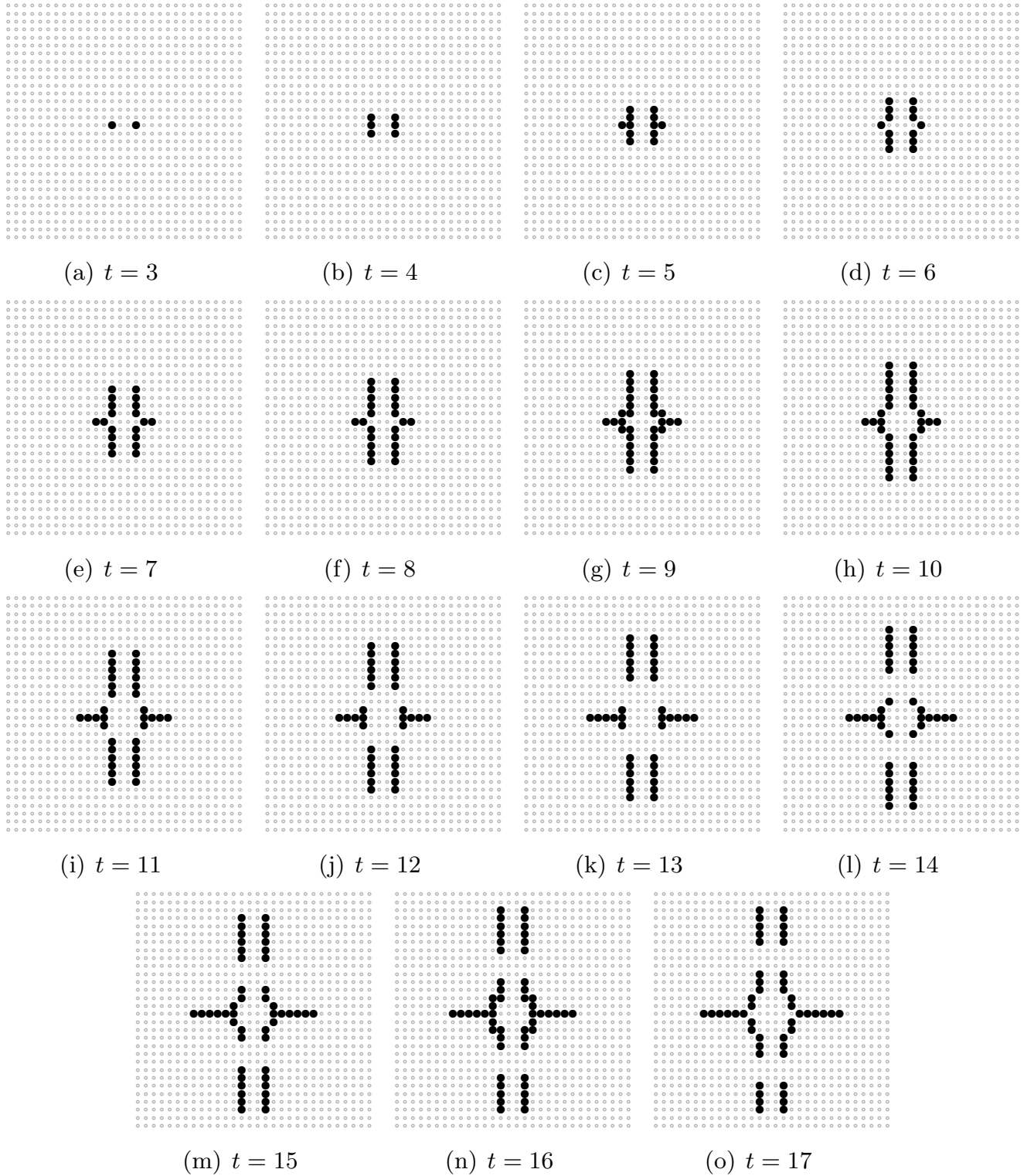


FIG. 9: Snapshots of a growing pattern of excitation developed from a seed of two neighbouring cells in excited state. Excited

FIG. 10: Snapshot of configuration of conductive cells developed from seed  $++$ .

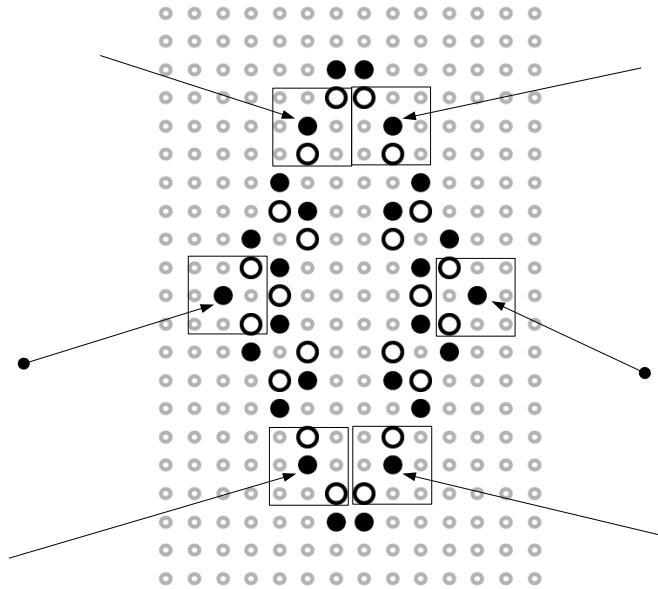


FIG. 11: Configuration of excited (●) and refractory cells (○) with highlighted cells responsible for formation of conductive pathways. Cells where double wire is formed are marked with arrows and single wire with arrows with disc tops. This configuration develops at seventh step of the seed's evolution, Fig. 9h.

refractory states:  $\begin{smallmatrix} \circ & \circ & - \\ \circ & \circ & + \\ - & + & \circ \end{smallmatrix}$  (Fig. 14a)ikmoqs). The particle travels south. Its tail leaves a trace of conductive cells (Fig. 14a)ikmoqs)jlnprt) due to excited cell having two refractory neighbours:  $\begin{smallmatrix} \circ & - & \circ \\ \circ & + & \circ \\ - & \circ & \circ \end{smallmatrix}$ , and therefore decreasing its  $\theta_1$  to 1.

We have undertook an exhaustive search on head on collisions between wires growing north and south (Fig. 15). A wire growing south was generated by seed  $\begin{smallmatrix} - & \circ \\ + & + \end{smallmatrix}$  and a wire growing north by seed  $\begin{smallmatrix} + & + \\ - & \circ \end{smallmatrix}$ . At the beginning of each run seeds were placed at distance  $C = (h, v)$  from each other, where  $h$  is a number of cells along rows and  $v$  along columns of cellular array (Fig. 15a). Types of collision outcomes discovered are also illustrated by schemes in in Fig. 16k–r. The following basic types are found.

For distance  $C = (80, 0)$  the wires collide, reflect and then retract back to their origin sites. After retraction the continuing growing directions opposite to their original velocity vectors. Wire originally growing north grows south, and wire growing south grows north (Fig. 15b). In the same time an additional growth seed is formed at the site of the collision between wires, it gives rise to two more wires growing north and south (Figs. 15b and 16k).

In situation of one-cell horizontal shift between seeds' positions, distance  $C = (80, 1)$ , both wires reflect but only the north growing wire (reflected south) continue growing beyond position of its original seed (Figs. 15c and 16l). If there is a two cell horizontal space between the seeds (Figs. 15d) then both wires reflect and continue their growth into reflected directions (Figs. 15d and 16m).

For distance  $C = (80, 3)$  both wires reflect as in previous situations, however only one wire continues growing north (after passing initial position of a seed) but second wire makes  $90^\circ$  turn when entering initial position of the its seed and then grows east (Figs. 15e and 16n). In situations  $C = (80, 4)$  both wires just reflect without forming any conductive bridges or patterns growing from the site of their collision (Figs. 15f and 16o). In situations  $C = (80, 5)$  and  $C = (81, 5)$  wires pass near each other without interacting (Figs. 15fm).

When distance between seeds is  $C = (81, 0)$  the growing wires reflect and detract back to their points of origination. However when they reach positions of their seeds a new pattern is formed there (Figs. 15h). It exhibits multi-thread wires growing north-west, south and east from the position of northern seed, and south-west, north and east from the position of southern seed (Fig. 16p).

An E-shaped configuration of three wires growing east is formed when  $C = (81, 1)$ ; the seeds' site are also connected by a conductive wire (Figs. 15i and 16q).

**Finding 4** By positioning seeds  $\begin{smallmatrix} + & + \\ - & \circ \end{smallmatrix}$  and  $\begin{smallmatrix} - & \circ \\ + & + \end{smallmatrix}$  with shift  $C = (\text{odd}, 2)$  it is possible to make a stationary conductive wire between the seeds' locations.

For example, in situation  $C = (81, 2)$  (Figs. 15j) the growing wires collide, make a conductive bridge and stop

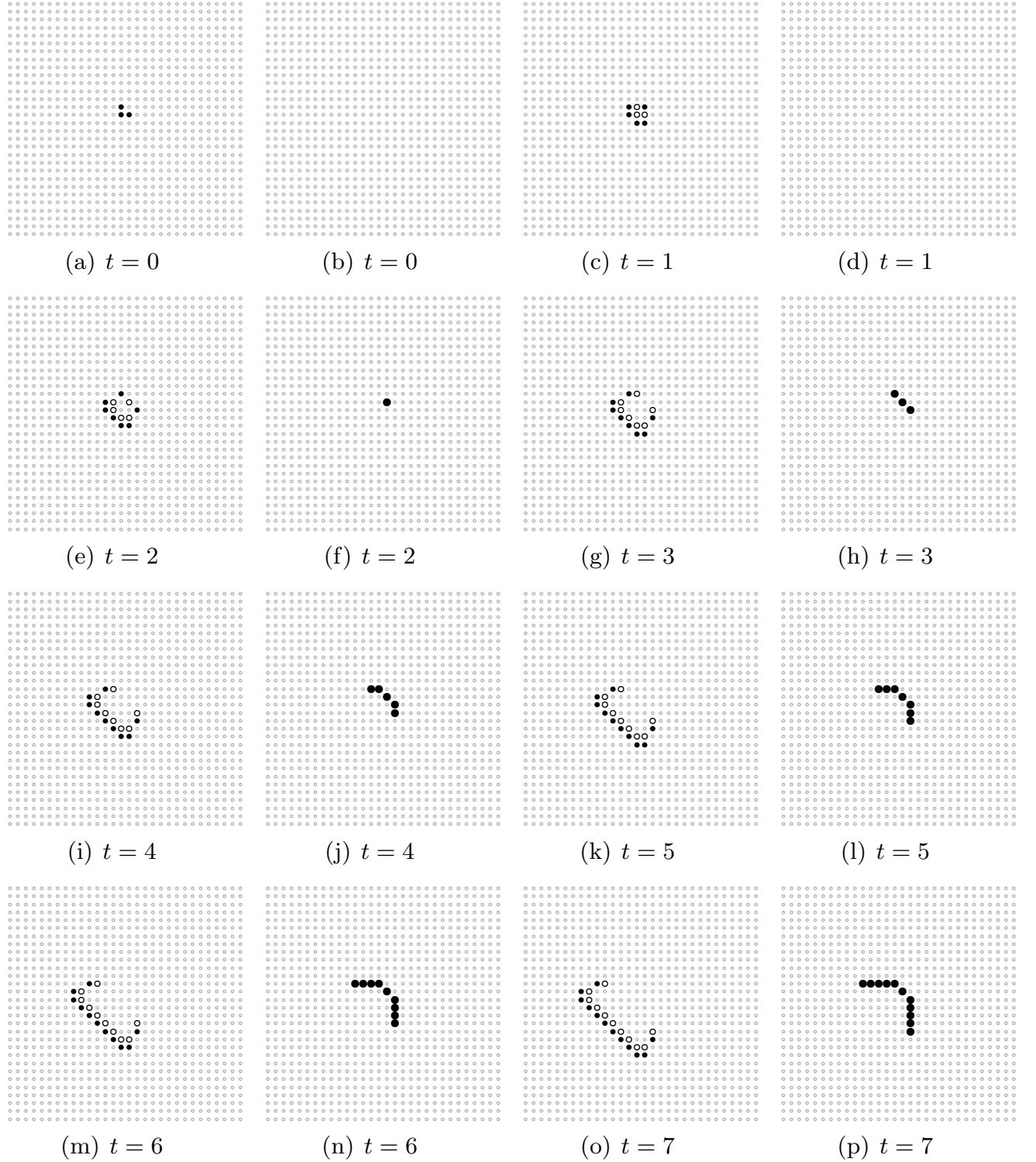
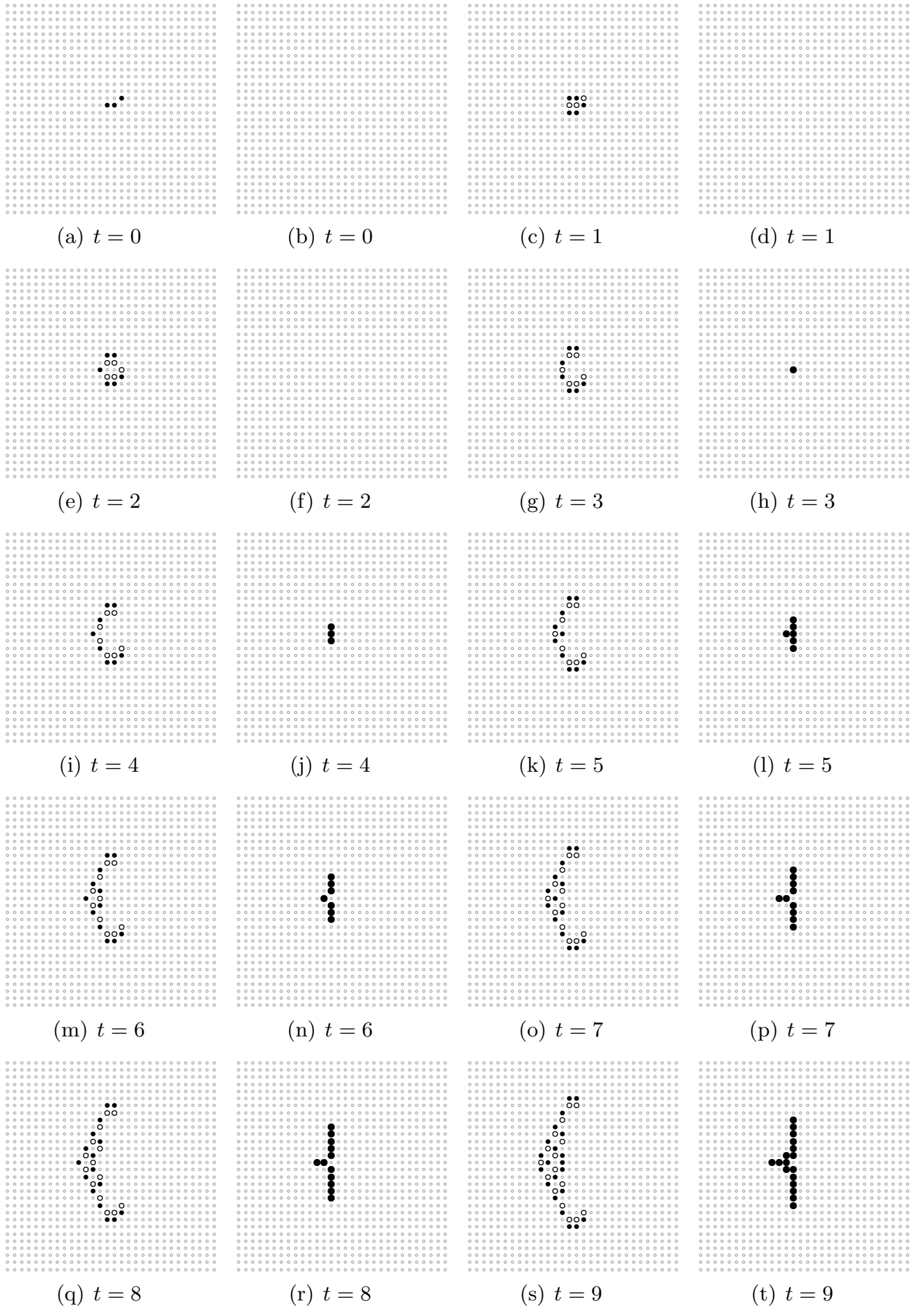


FIG. 12: Production of two wires growing east and south. For each time step  $t$  we show excitation (left pattern) and conductivity (right pattern) configurations. In the excitation configurations excited cells are solid black discs, refractory cells are circles. In the conductivity configurations conductive cells are black discs and non-conductive are grey dots.

FIG. 13: Three wires growing north, south and east. For each time step  $t$  we show excitation (left pattern) and conductivity

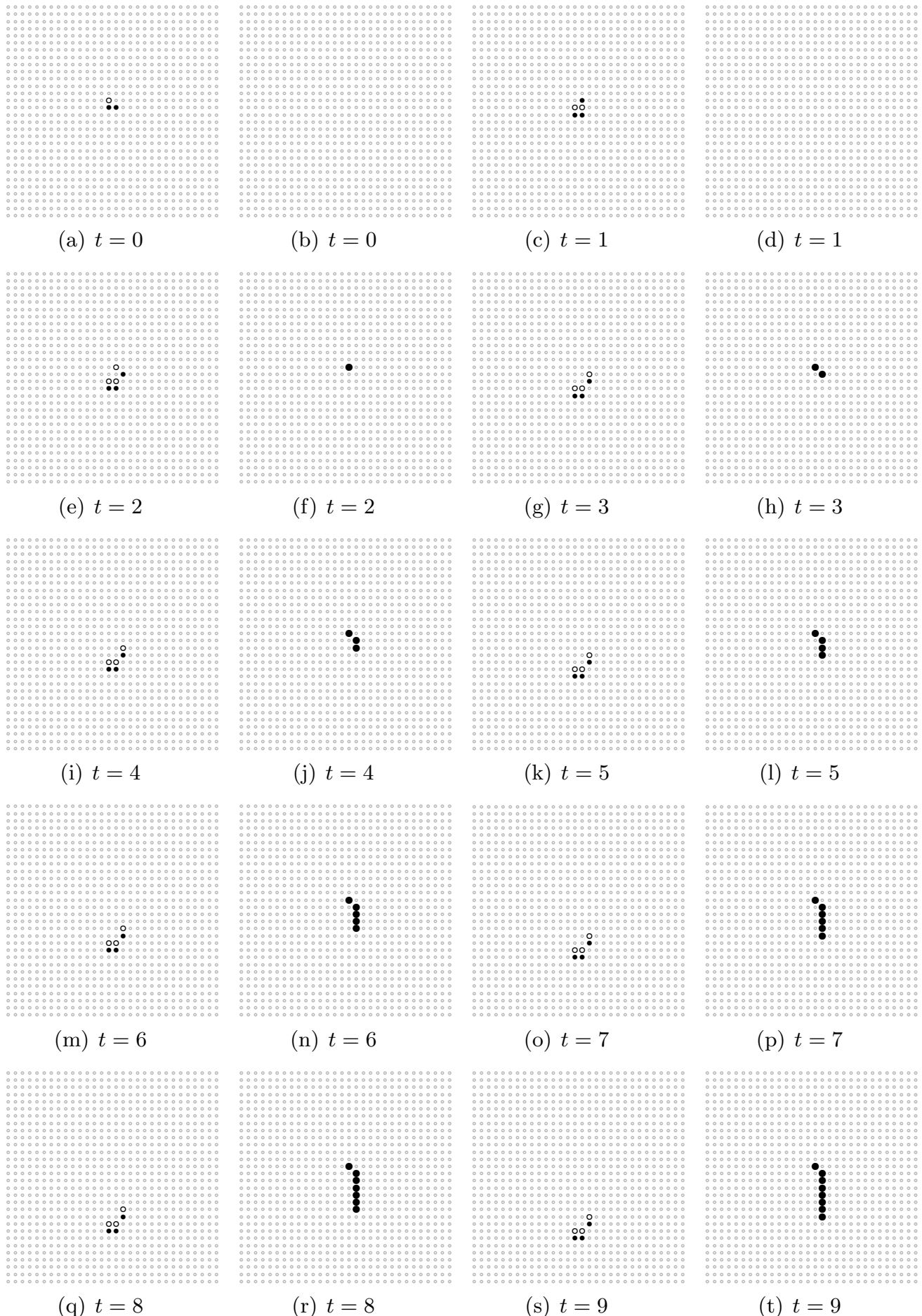


FIG. 14: Single wire grows south. For each time step  $t$  we show excitation (left pattern) and conductivity (right pattern) configurations. In the excitation configurations excited cells are solid black discs, refractory cells are circles. In the conductivity

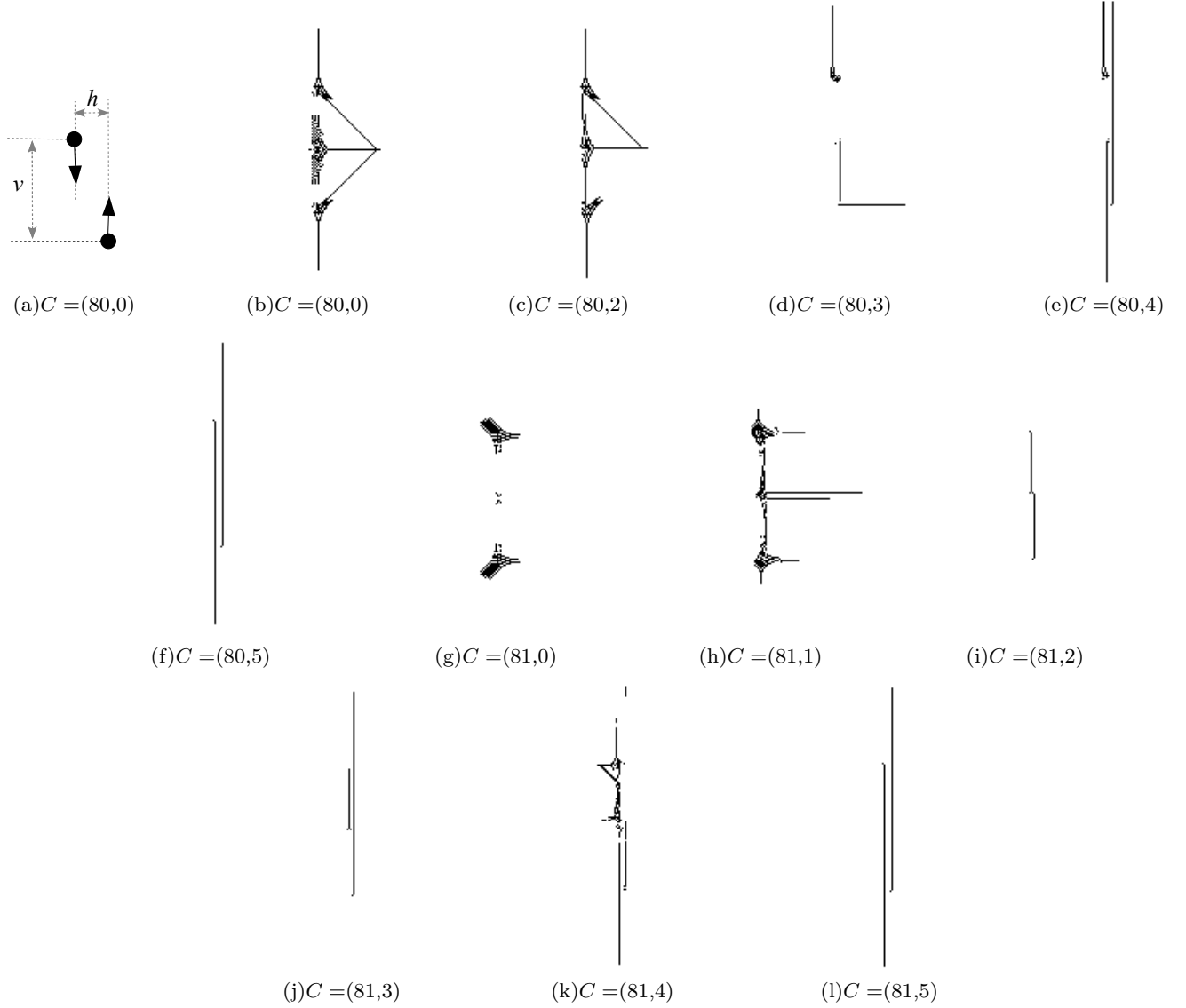


FIG. 15: Head on collision between wires growing north and south for various distances  $C = (h, v)$  between their seeds.  $h$  is a number of cells between westmost excited cells of seeds, and  $v$  is a number of cells between northmost excited cells of seeds. Snapshots of configurations of conductive states are taken at 270th step of iterations. The outcomes of collisions are the same for automata governed by functions  $E(1, 0, 0, 0)$  and  $E(1, -1, 0, 0)$ .

their propagation. Thus a stationary wire is formed connecting sites of southern and northern seeds (Fig. 16r). The seeds' sites are connected by a wire in  $C = (81, 3)$  (Figs. 15k) and  $C = (81, 4)$  (Figs. 15l) however the wire continue expanding north and south.

To study outcomes of side collisions between wires we position two seeds  $\begin{smallmatrix} + & + \\ - & + \end{smallmatrix}$  and  $\begin{smallmatrix} - & + \\ 0 & + \end{smallmatrix}$  at distance  $C = (h, v)$  (Fig. 17a), where  $h$  is a number of cells between northmost excited cells of seeds, and  $v$  is a number of cells between northmost excited cells of seeds. The seed  $\begin{smallmatrix} + & + \\ - & + \end{smallmatrix}$  leads to formation of a single thread wire growing north. The seed  $\begin{smallmatrix} - & + \\ 0 & + \end{smallmatrix}$  generates a wire east. Configurations of cells in conductive states developed on 300th step after excitation of automaton with the seeds are shown in Fig. 17.

Colliding wires stop short of touching each other and do not propagate anymore for  $C = (60, 40)$  and  $C = (61, 43)$  (Figs. 17bk and 16a). Growth of wire propagating north is cancelled by wire propagating east in  $C = (60, 42)$  (Fig. 16b), the wires do contact each other (Figs. 17c).

In condition  $C = (60, 43)$  (Figs. 17d) two new growing wires are formed in the result of collision of a wire travelling north to a wire travelling east. One new wire propagates west and another wire propagates east (Fig. 16c).

Three new growing wires are formed in collision of north and east propagating wires when distance between their

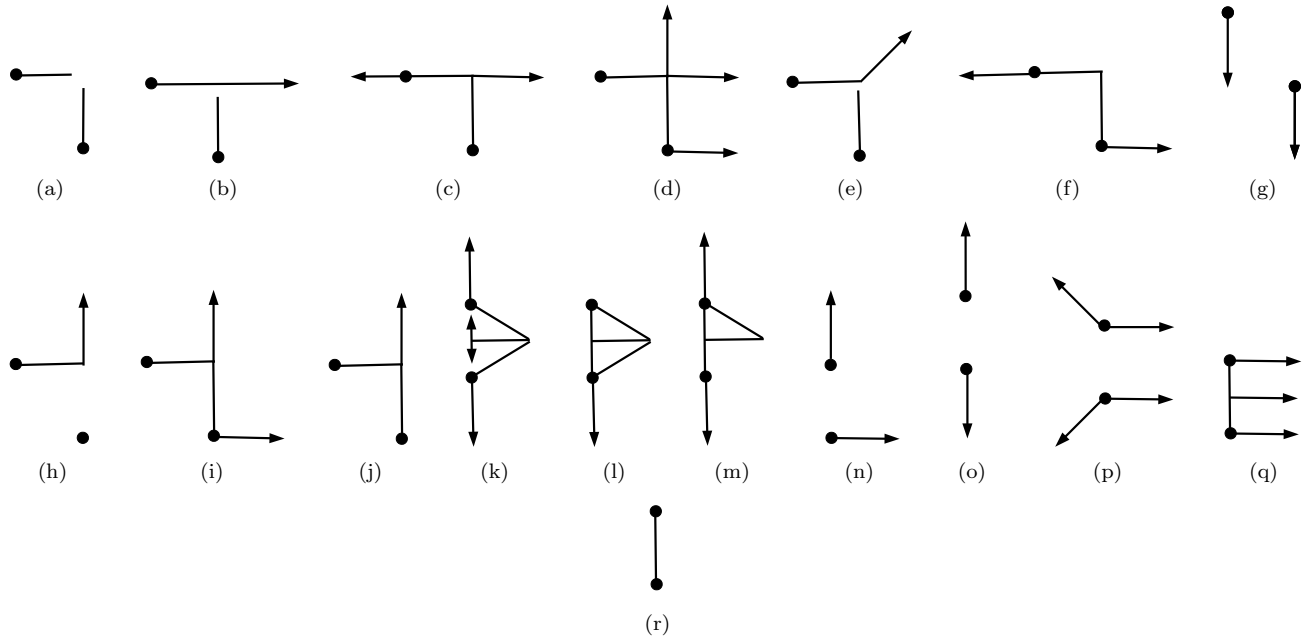


FIG. 16: Schemes of interactions between wires. Initial positions of seeds are shown by black discs. Non-growing wires are shown by line segments and growing wires by arrows. (a–j) side collision, (k–r) head on collision.

seeds is  $C = (60, 44)$  (Figs. 17e and 16d) and  $C = (61, 40)$  (Figs. 17g and 16d). One new wire propagates north and two new wires propagate east. The south wire propagating east is formed when originally north propagating wire retracts in the result of collision with originally east propagating wire and is reflected by configurations of excitation interval boundaries it imposed by itself.

Almost elastic like reflection of a wire is observed in case  $C = (60, 45)$  (Figs. 17f and 16e). A wire growing north collides and got cancelled by a wire growing east. In the result of impact the east growing wire is reflected and starts growing north-east (Fig. 16e).

In situation  $C = (61, 42)$  both wires retract in the result of collision. However, when they reach sites of their origination (where cells have already updated boundaries of excitation interval) they are transformed into extended patterns which give rise to two new wires, both growing south (Figs. 17g and 16j).

In situation  $C = (61, 44)$  and  $C = (61, 45)$  a wire growing north is retracted back to its seed's position in the result of collision with a wire growing east (Figs. 17h and 16h). In the same time the wire growing east is reflected and turns north.

**Finding 5** *It is possible to implement universal routing of conductive wires by positioning seeds of growing wires, the following operations with wires are implementable:*

- Formation of stationary wires (Fig. 16r)
- Stopping of both growing wires (Fig. 16a)
- Stopping of one wire by another wire without formation of conductive bridge (Fig. 16b)
- Formation of conductive circuit with one growing wire (Fig. 16l)
- Formation of conductive circuit with two growing wires (Fig. 16cfikm)
- Formation of conductive circuit with three growing wires (Fig. 16dq)
- Reflection of wires without conductive bridging (Fig. 16hno)
- Stopping of one wire and reflection of another (Fig. 16e)
- Co-orientation of both growing wires without formation of conductive bridge (Fig. 16g)
- Symmetric reflection and multiplication without formation conductive bridging (Fig. 16p).

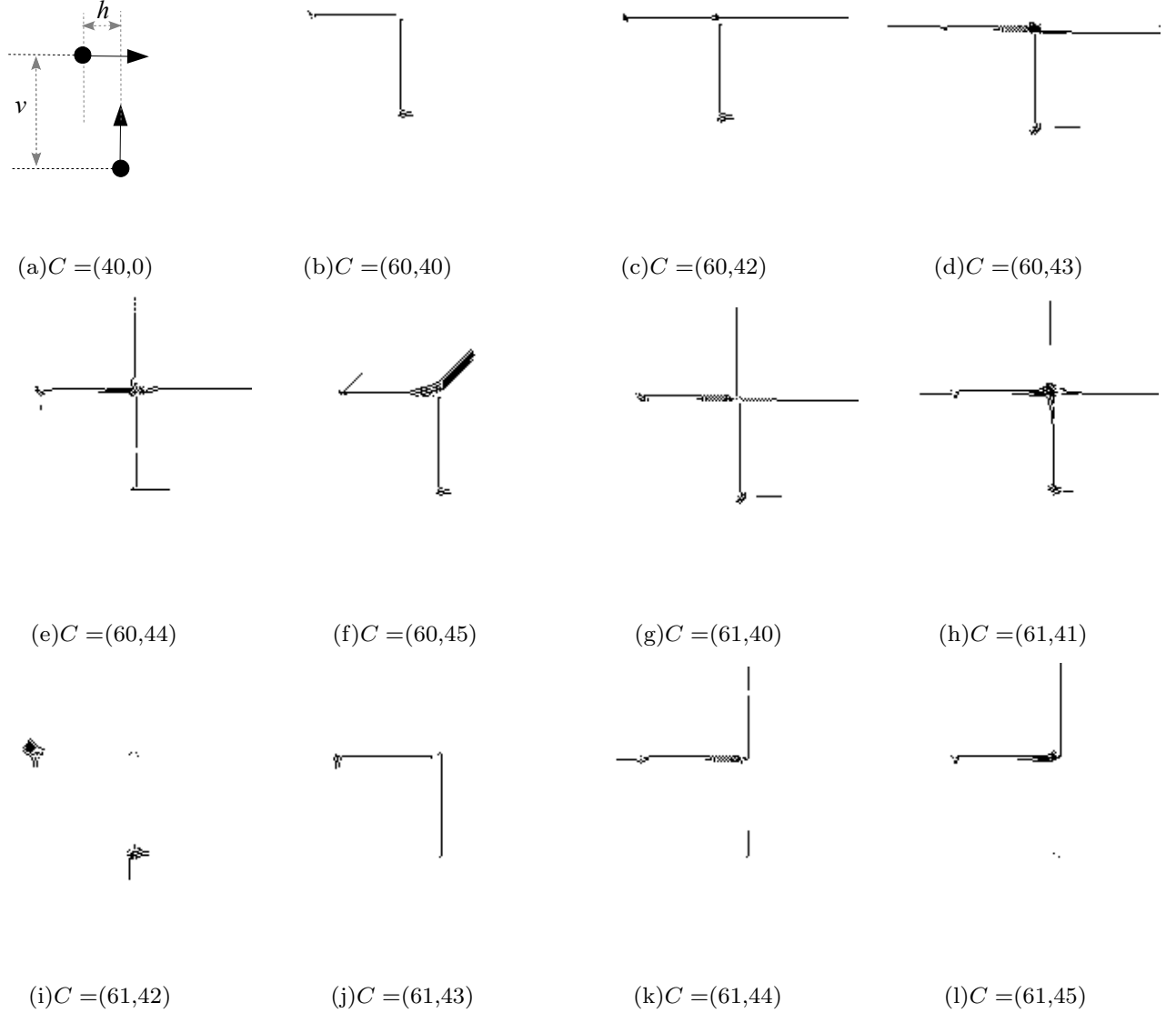


FIG. 17: Side collision between wires growing north and east for various distances  $C = (h, v)$  between their seeds.  $h$  is a number of cells between northmost excited cells of seeds, and  $v$  is a number of cells between northmost excited cells of seeds. Snapshots of configurations of conductive states are taken at 300th step of iterations. The outcomes of collisions are the same for automata governed by functions  $E(1, 0, 0, 0)$  and  $E(1, -1, 0, 0)$ .

## V. SUMMARY

We introduced a two-dimensional excitable cellular automaton where resting cells excite depending on whether numbers of their excited neighbours belong to excitation intervals and boundaries of the excitation intervals are updated depending on ratio of excited and refractory cells in each cell's neighbourhood. We defined conductivity of a cell via size of its excitation interval and selected the excitation interval update functions that lead to formation of connected configurations of conductive cells.

We demonstrated that by positioning elementary seeds of excitation we grow conductive wires (chains of cells in conductive states) and implement routing of the wires via collisions between the wires. Results presented might shade a light onto development of information pathways in excitable spatially extended media and contribute towards manufacturing of self-growing and self-organising circuits in ensembles of organic memristive polymers.

Principle findings of the paper are following:

- We demonstrated that it is possible to fine tune conductivity of an excitable medium by controlling local dynamics of excitation.
- Functions which stabilise excitation dynamics (where size of excitation interval increase with decrease of excitation and decreases when excitation dominates) generate fully conductive when a small number of initially resting cells are stimulated.
- A point-wise initial excitation can play a seed of a growing wire, a chain of cells in conductive states; directions of the wire grows in pre-programmed in the configuration of initial excitation
- The growing wires can be routed in almost arbitrary manner, dependent on positions of their seeds
- Several wires can interact with each other by changing directions of their growth, merging in a single wire and co-aligning.

We shown how to design and grow potential information pathways however we did not study how the information can be processed in the conductive configurations and circuits. In many cases of extended patterns are formed at the sites of collision between growing wires. Chances are high that these patterns can implement a range of sensible transformations input excitation to output excitation, which could be interpreted in terms of computation. Computational abilities of the conductive circuits grown in excitable cellular automata will be a major topic of further studies.

- 
- [1] Ilachinski A. Cellular Automata: A Discrete Universe (World Scientific, Singapore, 2001).
  - [2] Chopard B. and Droz M. Cellular Automata Modeling of Physical Systems (Cambridge University Press, 2005).
  - [3] Gerhardt M., Schuster H. and Tyson J. J. A cellular excitable media. *Physica D* 46 (1990) 392–415.
  - [4] Markus M. and Hess B. Isotropic cellular automata for modelling excitable media. *Nature* 347 (1990) 56–58.
  - [5] Adamatzky A., De Lacy Costello B., Asai T. Reaction-Diffusion Computers (Elsevier, Amsterdam, New York, 2005).
  - [6] Yang X. Computational modelling of nonlinear calcium waves. *Appl. Mathem. Modelling* 30 (2006) 200–208.
  - [7] Hartman H. and Tamayo P., Reversible cellular automata and chemical turbulence, *Physica D* 45 (1990) 293–306.
  - [8] Greenberg J. M. and Hastings S. P. Spatial patterns for discrete models of diffusion in excitable media, *SIAM Journal on Applied Mathematics* 34 (1978) 515–523.
  - [9] Adamatzky A. and Holland O. Phenomenology of excitation in 2D cellular automata and swarm systems. *Chaos, Solitons & Fractals* 3 (1998) 1233–1265.
  - [10] Adamatzky A. On diversity of configurations generated by excitable cellular automata with dynamical excitation intervals. *Int J Modern Physics C* (2012), in press.
  - [11] Chua L. O., Memristor — the missing circuit element. *IEEE Trans. Circuit Theory* 18 (1971) 507–519.
  - [12] Chua L. O. and Kang S. M., Memristive devices and systems. *Proc. IEEE* 64 (1976) 209–223.
  - [13] Chua L. O. Device modeling via non-linear circuit elements. *IEEE Trans. Circuits Systems* 27 (1980) 1014–1044.
  - [14] Williams R. S. How we found the missing memristor. *IEEE Spectrum* 2008-12-18.
  - [15] Erokhin V., Fontana M.T. Electrochemically controlled polymeric device: a memristors (and more) found two years ago. (2008) arXiv:0807.0333v1 [cond-mat.soft]
  - [16] Yang, J.J., Pickett, M. D., Li, X., Ohlberg, D. A. A., Stewart, D. R. and Williams, R.S. Memristive switching mechanism for metal-oxide-metal nanodevices. *Nature Nano*, 2008 3(7).
  - [17] Erokhin V., Schütz A., and Fontana M.P. Organic memristor and bio-inspired information processing. *Int J Unconventional Computing* 6 (2009) 15–32.
  - [18] Strukov, D.B., Snider, G. S., Stewart, D. R. and Williams, R. S., The missing memristor found. *Nature* 453 (2008) 80–83.
  - [19] Erokhin V., Howard D., Adamatzky A. Organic memristor devices for logic elements with memory. *Int. J. Bifurcation Chaos* (2012), in press.
  - [20] Itoh M. and Chua L. Memristor cellular automata and memristor discrete-time cellular neural networks. *Int. J. Bifurcation and Chaos* 19 (2009) 3605–3656.
  - [21] Adamatzky A. and Chua L. Memristive excitable cellular automata. *Int. J. Bifurcation Chaos* 21 (2011) 3083–3102.
  - [22] Adamatzky A. and Chua L. Phenomenology of retained refractoriness. *Int. J. Bifurcation Chaos* (2012), in press.
  - [23] Erokhin V., Berzina T., Smerieri A., Camorani A., Erokhina S., Fontana M.P. Bio-inspired adaptive networks based on organic memristors *Nano Communication Networks* 1 (2010) 108–117.
  - [24] Bode M., Liehr A. W., Schenk C. P., Purwins H.-G. Interaction of dissipative solitons: particle-like behaviour of localized structures in a three-component reaction-diffusion system. *Physica D* 161 (2002) 45–66.
  - [25] Grnert G., Dittrich P., Zauner K.P. Artificial wet neuronal networks from compartmentalised excitable chemical media. *ERCIM News* 2011 (85) 30-32.
  - [26] Adamatzky A., Holley J., Dittrich P., Gorecki J., De Lacy Costello B., Zauner K.-P., Bull L. On architectures of circuits implemented in simulated Belousov-Zhabotinsky droplets. *Biosystems* 109 (2012) 7277.

- [27] King P. H., Corsi J. C., Pan B.-H., Morgan H., de Planque M. R., Zauner K.-P. Towards molecular computing: Co-development of microfluidic devices and chemical reaction media. Biosystems 109 (2012) 18-23.
- [28] Szymanski J., Gorecka J. N., Igarashi Y., Gizynski K., Gorecki J., Zauner K.-P., Planque M. D. Droplets with information processing ability. Int J Unconventional Computing 7 (2011) 185–200.